Numerical approach to the dispersion of a pollutant discharge in a water table

Hami Khelifa[a],[*]

[a]*Laboratory of Environmental and Energy Systems LSEE, Institute of Science and Technology, University Center Ali KAFI, Tindouf, Algeria*

A R T I C L E   I N F O

A B S T R A C T

In the present study, simulations were carried out to determine the infiltration of a pollutant landfill in a homogeneous and isotropic slick. The system of basic equations, which govern the principle of conservation of the momentum coupled with Darcy's law, was developed to resolve the displacement of the pollutant in the water table studied as a function of time.The fields and profiles of the velocity and concentration were presented, the influence of the porosity and the permeability of the medium was taken into account to obtain the rate (%) of the water pollution concentration of the water table and their infiltration with respect to depth. The simulation results obtained show that for a porosity of 20% at the same time with infiltration rates of 1×10^{-5}, 2×10^{-5} and 3×10^{-5} successively the concentration of the pollution compared to a depth of 3 (m) is equal to the following values: 20%, 45%, and 70%.

1   Introduction

Soil contaminations can be diffuse or one-off. In diffuse contaminations, there are one or more dangerous compound, the concentrations of which vary little, and in most cases, the surfaces concerned are very extensive.

In general, contaminations are diffuse when pollutants are emitted [1]:

- • From non-stationary sources (automobiles).

- • From very extensive sources (product deposits in agriculture).

- • From a large number of sources (vehicles, domestic stoves).

In spot contamination of the soil, these are large quantities of pollutants in an area delimited by fences, buildings, and contaminated sites. Chemically, there are several groups of pesticides, which have different persistence. The total amount of chlorinated hydrocarbons, which have the highest persistence, and are still used today, exceeds that of the other groups [1]:

The highest nitrate concentrations are found in free water tables. Indeed, these, as opposed to confined water tables,

* Corresponding author. Tel.: +2130697527407.
E-mail address: hami.khelifa@cuniv-ak-tindouf.dz

are not protected by impermeable geological layers and are more or less vulnerable to surface pollution.

The types of aquifer permeability (crack permeability for limestones and eruptive rocks, the permeability of interstices for sands and sandstones) also play an important role with regard to vulnerability to surface contamination.

The depth of the water table in relation to the ground is also a significant vulnerability factor.

In the nitrogen cycle, nitrates are formed from ammonium ion (NH3) under the action of aerobic bacteria in an oxidizing environment. Due to their positive charge, ammonium ions can have an affinity with clay minerals and therefore be adsorbed by clay [2]. As with ammonium, nitrates have a high solubility in water, but conversely, they interact very little with soils. For these reasons, nitrates have a high leaching potential. The transformation of nitrates into molecular nitrogen (N2) by denitrification occurs naturally by bacterial degradation under anaerobic and reducing conditions [3]. Denitrification is thought to be an important factor in the degradation of nitrates, but their attenuation in groundwater may also be due to dilution of surface water, irrigation water, and precipitation [4-6]. Often described as biological, denitrification could also be chemical in a strongly reducing medium to high concentrations of ferrous ions [7], for example in the presence of environments rich in pyrite. Some authors define a half-life for nitrates in an aquifer to represent denitrification. [8] For example, use a half-life of 2.3 years. In some cases, the instability of nitrates depending on the physical-chemical conditions of the environment may prevent their use as an inert tracer of pollution in groundwater from then on the surface [9].

In general, oxidizing conditions in an unsaturated zone are favorable for the nitrification of ammonium and then for the leaching of nitrates into the aquifer. Then, the oxidation-reducing conditions of the aquifer may or may not be conducive to denitrification. The fine grain size of the soils would make the nitrate leaching conditions less favorable [10] and could lead to significant denitrification when the medium becomes reduced [11]. The mineral load of groundwater (represented by electrical conductivity) can in some cases be inversely proportional to the occurrence of nitrates. Once circulating in the aquifer, the nitrate concentration in groundwater would be likely to be attenuated either because of the increased time for degradation or by a dilution effect [10]. Temporal fluctuations of nitrates in groundwater relative to climate seasonality and fertilization periods may also occur. There may be a supply of nitrates directly following the periods of fertilization and a rapid flow following irrigation or significant rainfall, or conversely, a dilution of the concentrations in the aquifer by a recharge free of nitrates, as by example during the fall, outside the fertilization period.

The occurrence of nitrates in the study area is low and no acceptance of the potability standard (10 mg N-NOi L) was observed. Low nitrate concentrations are observed downstream of the basin, but the highest (maximum 6.1 mg N-N03 / L) are found in Appalachian Piedmont. Concentrations less than 1 mg / L N-N03 may be natural, those between 1 and 3 mg / L N-N03 may be anthropogenic, while those greater than 3 mg / L N-N0 3 are certainly of anthropogenic origin [12].

After this bibliographical presentation on the subject where we cited above some works on basic concepts of groundwater pollution. In this present work, we propose a numerical (2D) approach to the dispersion of a polluting discharge in a homogeneous and isotropic captive water table. The determination of the problem posed is carried out by the mathematical resolution of the basic Navier-Stokes equations, which express the principle of conservation of the momentum coupled by the Darcy equation, which expresses the permeability of the medium studied.

2 Methodology

2.1 Physical model

The porous medium studied in this work presents a homogeneous and isotropic subsoil of 3 (m) of depth saturated with water, influenced by the infiltration of a polluting discharge of velocity V_{inf} which is worth: 1×10^{-5} (m/s). The influence of several Spatio-temporal physical parameters are taken into account to interpret the one in relation to the other of the study problem, The modeling of this problem was completed by the numerical resolution of the basic equations of the Navier-Stockes flow coupled by the Darcy equation to determine the field of the infiltration of the polluting discharge, and the differential equation of the concentration to calculate the variation of the rate in (%) of this concentration from the top to the bottom of the subsoil is studying.

2.2 Mathematical model

Darcy's law was established under specific flow conditions, which limit its validity. The main underlying assumptions are [13,14]:

- Homogeneous, isotropic and stable solid matrix ,Homogeneous,
- isothermal and incompressible fluid,
- Negligible kinetic energy,
- Laminar flow (Darcy flow: Re << 1),
- The spatial variations in density (compressibility, heterogeneity) and viscosity (temperature) of the liquid phase are small enough that their effect can generally be neglected.

2.2.1 Equations of the problem

Equation of the continuity:

$$\frac{\partial u}{\partial x} = \frac{\partial v}{\partial y}$$

(1)

Porous media are modeled by adding momentum source terms of the fluid flow equation described as equations (2) and (3). Darcy's law considers the source term in these two equations. $\frac{\mu_f}{k}u$, and $\frac{\mu_f}{k}v$: are the source terms for the directions (X, Y) in the momentum equations (2) and (3).

Equation of flow along the X-axis:

$$\frac{\partial u}{\partial t} + \rho_f \left(\frac{u}{\phi^2}\frac{\partial u}{\partial x} + \frac{v}{\phi^2}\frac{\partial u}{\partial y} \right) = -\frac{\partial p}{\partial x} + \frac{\mu_f}{\phi}\left(\frac{\partial^2 u}{\partial x^2} + \frac{\partial^2 u}{\partial y^2} \right) - \frac{\mu_f}{k}u$$

(2)

Equation of flow along the Y-axis:

$$\frac{\partial v}{\partial t} + \rho_f \left(\frac{u}{\phi^2}\frac{\partial v}{\partial x} + \frac{v}{\phi^2}\frac{\partial v}{\partial y} \right) = -\frac{\partial p}{\partial y} + \frac{\mu_f}{\phi}\left(\frac{\partial^2 v}{\partial x^2} + \frac{\partial^2 v}{\partial y^2} \right) - \frac{\mu_f}{k}v$$

(3)

With:
- k: coefficient of the permeability of the porous medium;
- ϕ : porosity of the medium ;
- ρ : density of the fluid ;
- μ : dynamic viscosity of the fluid.

Equation of concentration:

The transport of the polluting discharge takes place through convection and mass diffusion, and the equation of this transport in differential form is written:

$$\frac{\partial C}{\partial t} + \left(\frac{v}{\phi^2}\frac{\partial C}{\partial x} + \frac{v}{\phi^2}\frac{\partial C}{\partial y} \right) = \frac{D}{\phi}\cdot\left(\frac{\partial^2 C}{\partial x^2} + \frac{\partial^2 C}{\partial y^2} \right)$$

(4)

Or:
- C: concentration of the pollutant,
- v: flow velocity along the Y-axis.
- D: coefficient of molecular diffusivity.

Boundary conditions:

The four boundary conditions of the present study are shown in figure 1:

- Wall (1): permeable rock (imposed pollutant discharge, $C = 100$ %), the infiltration velocity $V_{inf} = 1\text{x}10^{-5}$ (m/s) ;
- Wall (2): permeable rocks (conditions of infinite symmetry);

- Wall (3): impermeable rock ($C = 0$ %, $V = 0$ (m/s));
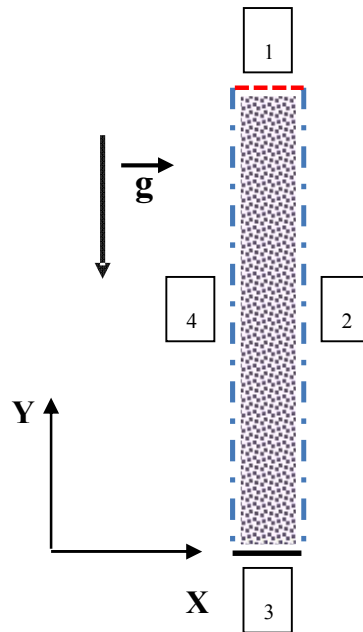- Wall (4): permeable rocks (conditions of infinite symmetry).

Fig. 1 – Physical model studies.

3 Simulation procedures

3.1 Mesh test

We are therefore interested here in a (2D) numerical problem. For a gradually varied flow, great longitudinal distances are necessary to observe significant variations in height; in areas where the flow is rapidly changing, the meter is an acceptable longitudinal length scale. As the simulation is performed on a homogeneous and isotropic water-saturated subsoil 3 (m) deep, we can expect a realistic solution, placing a compute node every centimeter. Then, we chose increasingly coarser meshes.

The superposition of the velocity profiles along the (X) axis for the three different meshes figure 2. Represents the same pace, that is to say the same physical behavior with a very small offset between each other thanks to the calculation errors due to the interpolation adopted to simulate the present problem, the speed simulated at the level reference plane 2 (m) deep has the following value: $u = (2 \pm 0.04) . \times 10^{-6}$ (m/s). We thus note that the numerical solution is all the closer to reality as the mesh is fine. We can then relate the deviations (to the physical solution) observed to the very principle of resolution by the finite volume method (MVF). The idea of this method is to fix the solution to known values on the nodes. Next, we build the final solution by interpolating between each node. So, choosing a fine mesh means that we have a good knowledge of the solution we want to obtain. Conversely, for a coarse mesh, we then have a more approximate idea of the solution to be obtained. We do not know how in practice an interpolation is carried out, but we think that this one is done without taking into account the physical solution between two nodes.
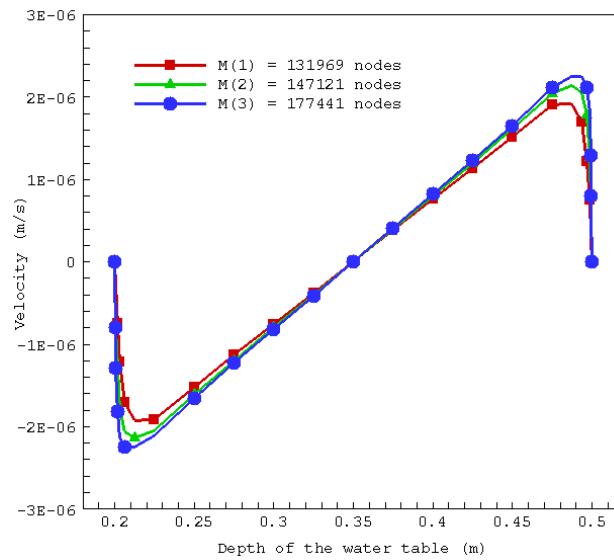
Fig. 2 –Mesh test.

We noted the value of the resulting velocity of the flow for each of the solutions. We found residuals in the same order of magnitude when we expected to have large residuals for the coarse meshes. In conclusion, if we increase the number of nodes, then we decrease the errors due to interpolations between nodes, and the numerical solution is closer to reality. We also noted that the computation time increases with the fineness of the mesh, but this increase is not significant for the meshes chosen in our simulations (Error < 0.2 %), table 1.

Table 1 - Calculation of the simulation error for various meshes.

Cases studied	Number of nodes	Velocity (m/s)	Error (%)
M (1)	131969	4.940×10^{-5}	-
M (2)	147121	4.931×10^{-5}	0.18
M (3)	177441	4.929×10^{-5}	0.04

3.2 Convergence test

The evolution of the concentration C over the time of the simulation in a horizontal plane on the free surface of the studied subsoil is represented in figure 3. This figure comprises two successive phases, the transient phase which depends strongly on l 'initial state of the system: $C_0 = 0$ (%) and V0 = 0 (m / s) where the digital solution is unstable and the phase of the stationary regime which is independent of the initial state of the system: $C = 100$ (%) and $V_{inf} = 1 \times 10^{-5}$ (m/s) in which our digital solution has become permanent. The results obtained affirm a passage between an initialcomputation time towards an inertial computation time of the system.
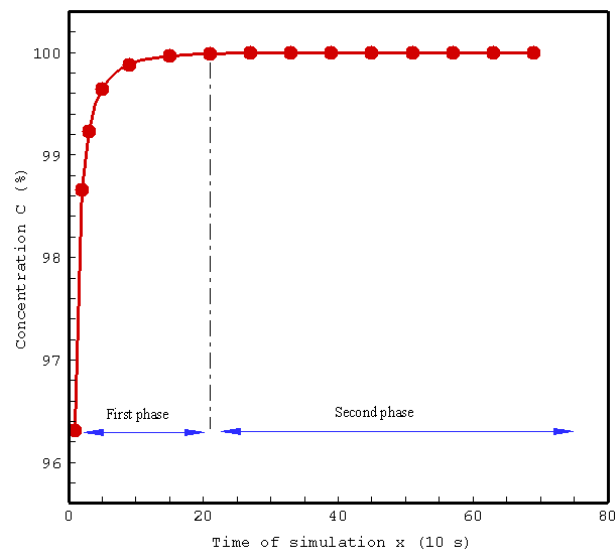
Fig. 3 –Convergence test.

4   Results and discussion

The concentration field over time for a homogeneous and isotropic subsoil influenced by the vertical infiltration of a polluting landfill is shown in figure 4, the maximum value of this concentration C is equal to: 100 (%) at the level of the free area of the basement. By the effect of gravity, these polluting discharges flow downwards from the subsoil with decreasing values with respect to the depth.
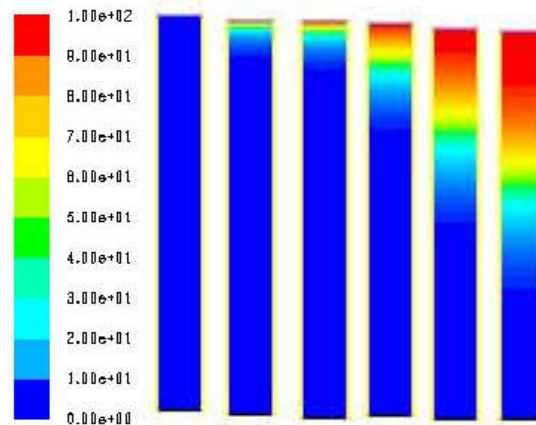

Fig. 4 – Concentrationfield over time for a porosity of 20% for: t = 1x1800 (s), 10x1800 (s), 20x1800 (s), 30x1800 (s), 40x1800 (s), and 50x1800 (s).

Figure. 5 represents the profile of the concentration of the polluting discharge over time. For a simulation time, which is equal to: 10x1800 (s), the polluting discharge moves vertically towards 1 (m) of depth with a velocity $v = 1x10^{-6}$ (m / s) and 2 (m) of depth with a velocity $v = 2x10^{-6}$ (m / s) for a time which is equal to 5 times the initial time.
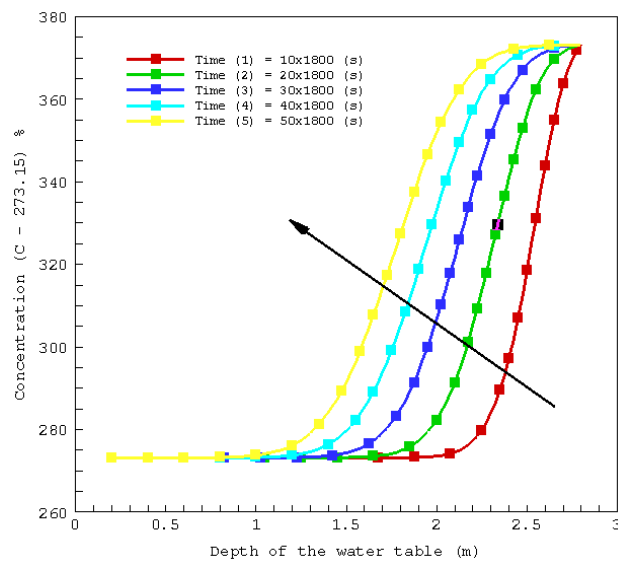
Fig. 5– Concentration profiles over time for a porosity of 20% for: t = 1x1800 (s), 10x1800 (s), 20x1800 (s), 30x1800 (s), 40x1800 (s), and 50x1800 (s).

Figure 6 represents the infiltration velocity with respect to a horizontal reference surface in the middle of the zone studied, we notice that the velocity increases by ($1x10^{-6}$ - $2.5x10^{-6}$) by the increase in the porosity of the medium, positive and negative values indicate the symmetry of the medium being studied (it's a sign convention).
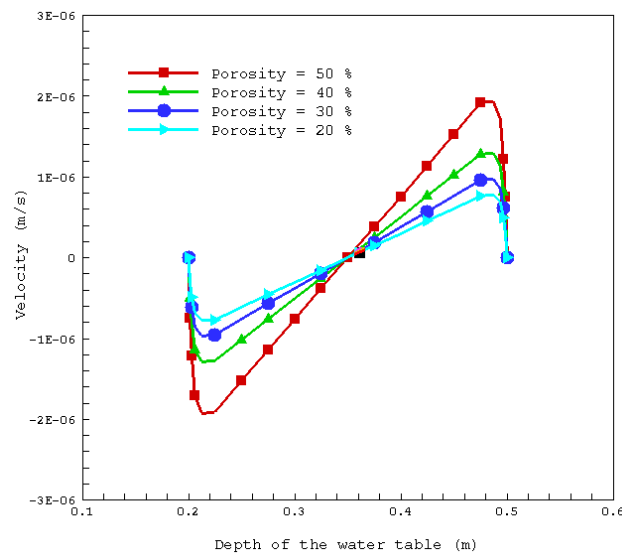

Fig. 6 – Velocity profiles as a function of porosity for: t = 20x1800 (s).

The comparison between the three cases of the transport of the pollutant discharge as a function of the infiltration feed rate for a time, which is worth 20x1800 (s) has been presented in figure 7, so the higher the vertical filtration speed, the more the displacement of the polluting dump is considerable. The speeds taken into account are: $1x10^{-5}$ (m / s), $2x10^{-5}$ (m / s) and $3x10^{-5}$ (m / s).
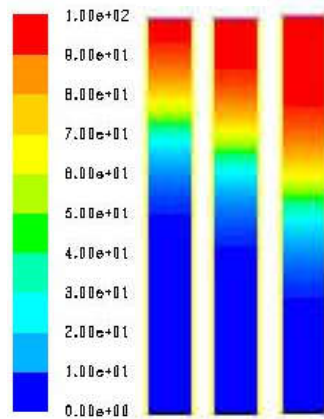
Fig. 7 – Concentration field as a function of the feed rate for: t = 20x1800 (s), V_{inf} = 1x10^{-5} (m/s), 2x10^{-5} (m/s), and 3x10^{-5} (m/s).

Figure 8 shows the concentration profile as a function of the rate of infiltration. Note that the displacement of the pollutant discharge to a depth increases with the increase in the rate of infiltration. For the case, simulate in a: 1 (m), 1.5 (m) and 2 (m) depth successively for infiltration velocity's of values: 1x10^{-5} (m/s), 2x10^{-5} (m/s) and 3x10^{-5} (m/s).
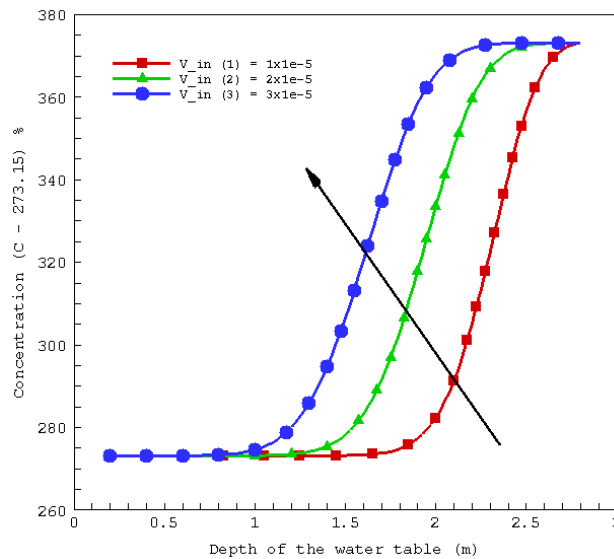

Fig. 8 – Concentration profiles depending on the feed rate for t = 20x1800 (s), $V_{inf=}$ 1x10^{-5} (m/s), 2x10^{-5} (m/s), and 3x10^{-5} (m/s).

5   Conclusion

Numerical simulations were carried out numerically to determine the physical behavior of the displacement of a polluting discharge in a subsoil saturated with water, the modeling of this problem was based on the equations of the Navier-Stockes flow which govern the principle of conservation of motion coupled by the Darcy equation, which expresses the infiltration into the same environment and the differential equation of the concentration to find the rate in (%) of this pollutant in the studied domain. This simulation made it possible to make a parametric study on the vertical displacement of the pollutant discharged over time on the one hand and according to other physical parameters such as the infiltration velocity (1x10^{-5} (m/s), 2x10^{-5} (m/s) and 3x10^{-5} (m/s)) and on the other hand parameters concerning the medium such as permeability and porosity. The simulation results obtained show that for a porosity of 20% at the same time with infiltration rates of 1x10^{-5}, 2x10^{-5} and 3x10^{-5} successively the concentration of the pollution compared to a depth of 3 (m) is equal to the following values: 20%, 45%, and 70%.

REFERENCES

[1] Guillaume Meyzonna, 2012 .Estimation de la vulnérabilité de l'aquifère au roc de la zone bécancour (centre-du-québec). Mémoire présenté comme exigence partielle de la maîtrise en sciences de la terre, 141 p.

[2] Hajhamad, L., Almasri, M.N., 2009. Assessment of nitrate contamination of groundwater using lumped-parameter models. Environmental Modelling & Software, 24, 1073-1087.

[3] Appelo, C.A.J., Postma, D., 2005. Geochemistry, Groundwater and Pollution, 2nd ed. A.A. Balkema Publishers, Leiden, The Netherlands, 649 p.

[4] Bekesi, G., McConchie, J., 2002. The use of aquifer-media characteristics to model vulnerability to contamination, Manawatu region, New Zealand. Hydrogeology Journal, 10, 322–331.

[5] Chowdhury, S.H., Kehew. A.E., Passero, R.N, 2003. Correlation between nitrates contamination and ground water pollution potential. Ground Water, 41 (6), 735-745.

[6] Stigter, T.Y., Ribeiro, L., Carvalho Dill, A.M.M., 2006. Application of a groundwater quality index as an assessment and communication tool in agro-environmental policies- two Portuguese case study. Journal of Hydrology, 327, 578– 591.

[7] Andersen L.J., Kelstrup, N., Kristiansen, H., 1980. Chemical profiles in the Karup water-table aquifer, Denmark. Nuclear Techniques in groundwater pollution research, IAEA, Vienna, Austria, 47-60.

[8] Frind, E.O., W.H.M. Duynisveld, O. Strebel, and J. Boettcher, 1990. Modeling of Multicomponent Transport With Microbial Transformation in Groundwater: The Fuhrberg Case. Water Resources Research, 26, 1707-1719

[9] Verstraeten, I.M., Fetterman, G.S., Meyer, M.T., Bullen, T., Sebree, S.K., 2005. Use of tracers and isotopes to evaluate vulnerability of water in domestic wells to septic waste. Ground Water Monitoring and Remediation, 25(2), 107–117.

[10] Andrade, A.I.A.S.S., Stigter, T.Y., 2009. Multi-method assessment of nitrates and pesticides contamination in shallow alluvial groundwater as a function of hydrogeological setting and land use. Agricultural Water Management, 96, 1751–1765

[11] Rajmohan, N., Elango, L., 2005. Nutrient chemistry of groundwater in an intensively irrigated region of southern India. Environmenetal Geology, 47, 820–830.

[12] Larocque, M., Pharand, M.C., 2010. Dynamique de l'écoulement souterrain et vulnérabilité d'un aquifère du piémont appalachien (Québec, Canada). Revue des sciences de l'eau, vol. 23 n°1. p. 73-88.

[13] Hami Khelifa, Zeroual Ibrahim, 2017. Numerical approach of a water flow in an unsaturated porous medium by coupling between the Navier–Stokes and Darcy–Forchheimer equations. Latvian Journal of Physics and Technical Sciences, 54(6)., DOI:10.1515/lpts-2017-0041.

[14] Hami Khelifa, Talhi Abdelkrim, Zeroual Ibrahim, Modélisation d'un Ecoulement de Darcy dans un Milieu Poreux saturé. 3ème Conférence internationale sur la Mécanique des Matériaux et des Structures, 13, 14 et 15 Novembre2019, Marrakech, MAROC.

Nomenclature

- C concentration of the pollutant   (%)
- D: coefficient of molecular diffusivity   (m²/s)
- k :   coefficient of the permeability of the porous medium   (m/s) ;
- p: pressure   (Pa)
- u::   flow velocity along the X-axis   (m/s)
- v: flow velocity along the Y-axis.   (m/s)

Greek symbols

- ϕ :   porosity of the medium   (%)
- ρ :   density of the fluid   (Kg/m³)
- μ :   dynamic viscosity of the fluid   (Pl).